UNITED NATIONS EDUCATIONAL, SCIENTIFIC AND CULTURAL ORGANIZATION
INTERNATIONAL ATOMIC ENERGY AGENCY
INTERNATIONAL CENTRE FOR THEORETICAL PHYSICS
I.C.T.P., P.O. BOX 586, 34100 TRIESTE, ITALY, CABLE: CENTRATOM TRIESTE

H4.SMR/994-20

SPRING COLLEGES IN COMPUTATIONAL PHYSICS

19 May - 27 June 1997

TIME DEPENDENT METHODS IN QUANTUM MECHANICS I & II

R. COALSON
University of Pittsburgh
Department of Physics
Pittsburgh, Pennsylvania 15260
U.S.A.

Chapt. 1: Semiclassical Collision Theory, Gaussian Wavepacket Dynamics, and Driven Oscillators

1 A Problem in Semiclassical Collision Theory

Imagine a collision between an atom and a molecule. The molecule has rotational and vibrational degrees of freedom. In general the rotational and vibrational states of the molecule will be altered as a result of the collision. Transitions between internal states of a molecule induced by collisions with other atoms, molecules (or photons) are called "inelastic transitions". The principles of quantum mechanics enable us to predict the probabilities of "inelastic transitions", and both the theoretical framework for understanding such processes and a practical methodology for analyzing them are given in terms of wavepacket motion.

A wavepacket is simply a spatially localized wavefunction which evolves in time. To give a specific illustration, take a simplified version of the atom/molecule collision. Let us consider the collinear collision of a free atom with an atom bound by a spring to a wall. Realistically, the bound atom could be an atom on the edge of a solid surface. Or we can think of this as representing the vibrational motion of a diatomic molecule which is hit "end on" by a free atom. The situation is summarized in Fig. 1. This prototypical inelastic collision problem involves two degrees of freedom: the position of the bound atom (relative to its equilibrium position) will be labelled by x, and the position of the free atom by y. Even for such a simple scattering process, the quantum mechanical (S-matrix) theory is nontrivial. We shall defer a full treatment to Chapt. 3.

Here we adopt a simple semiclassical model that focusses on the vibrational motion of the bound atom. We thus consider a Hamiltonian with only one dynamical degree of freedom, x. The influence of the free atom is represented by an appropriate time-dependent force that drives inelastic (vibrational) transitions in the oscillator. One way to do this is to replace the full interaction potential $V_{int}(x,y)$ by the effective potential $V_{int}(x,y(t))$, where $y(t)$ is an imposed trajectory for the free atom. To find an appropriate trajectory we can freeze the vibrating coordinate at its equilibrium position and solve Newton's Equation for the "collision coordinate" evolution. For example, suppose the interaction potential is $V_{int}(x,y) = A\exp[-(y-x)/L]$, i.e., a simple repulsive interaction with strength A and interaction distance L. Then,

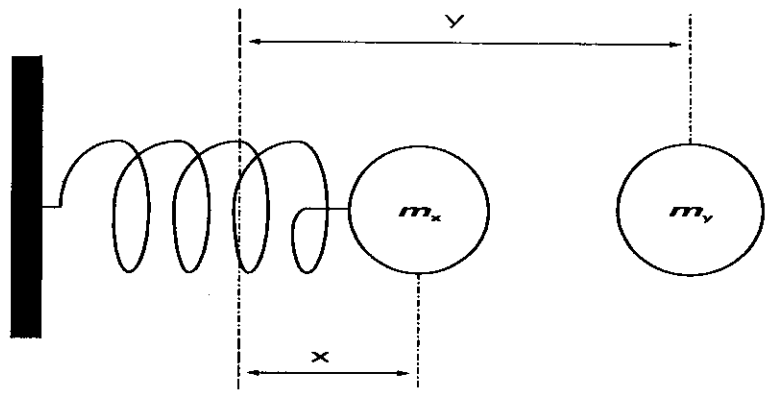

Figure 1: Collinear collision of projectile and particle attached to spring.

$$V_{int}(x, y(t)) \cong Ae^{-y(t)/L}[1 + x/L + ...] \tag{1}$$

where the expression in brackets is obviously the Taylor expansion of $e^{x/L}$. If the spring is sufficiently stiff the range of x is restricted to values near $x = 0$, so the Taylor series can be truncated after the first order term. Thus, operationally, we have

$$V_{int}(x, t) = f(t)x \tag{2}$$

with

$$f(t) \equiv \frac{A}{L}e^{-y(t)/L} \tag{3}$$

Note that $f(t)$ is (minus) the force exerted by the projectile on the oscillator when the oscillator is clamped at $x = 0$. In any case this function "forces" transitions between vibrational states of the oscillator. Typically, the force function would be a pulse peaking at certain (arbitrary) time and characterized by a certain strength and duration. A form which is easily rationalized is:

$$f(t) = \frac{m_y v_0^2}{2L}e^{-v_0^2(t-t_0)^2/L^2} \tag{4}$$

Here m_y is the projectile mass, v_0 is its initial incident velocity and t_0 the (arbitrary) "instant" of the collision. As is seen from the equation, the duration of the pulse is roughly L/v_0 and the maximum force is $m_y v_0^2/2L$, i.e. the potential energy difference between the asymptotically

free state and the state of maximum interaction (smallest y value) divided by the distance scale over which this change takes place.

Given preparation of the oscillator in vibrational eigenstate v, what is the probability after the collision that it will be in vibrational eigenstate v'? For simplicity, let us assume that the system is initially in $v = 0$ (unexcited), and notate the ground state Gaussian wavepacket of the oscillator by $\psi(x, 0)$. We wish to evolve this packet under the (time-dependent) potential indicated above so that after time t it becomes $\psi(x, t)$. Then we can overlap $\psi(x, t)$ with the harmonic oscillator eigenstate v' and compute the probability to be in state v' at time t:

$$P_{v'} = | < v'|\psi(t) > |^2 \tag{5}$$

We expect that after the collision, $P_{v'}$ will attain a well defined asymptotic value. To calculate these quantities we can utilize Gaussian Wavepacket Dynamics.

2 (Thawed) Gaussian Wavepacket Dynamics in 1-d

We present here the equations of motion for Thawed Gaussian Wavepacket Dynamics (GWD) in one spatial dimension [1]. We presume the particle is prepared in an initially Gaussian state. We then *assume* that the system remains a Gaussian for all times, so that its wavefunction can be represented by:

$$\psi(x, t) = \exp\left\{\frac{i}{\hbar}\left[\alpha_t(x - x_t)^2 + p_t(x - x_t) + \gamma_t\right]\right\} \tag{6}$$

Here, by construction we have $< \psi(t)|\hat{x}|\psi(t) >= x_t$, i.e. x_t is the position-space center of the wavepacket. Similarly, p_t is the momentum expectation value of the wavepacket state, $< \psi(t)|\hat{p}|\psi(t) >= p_t$. Of course, x_t and p_t are real-valued parameters. The complex-valued parameter α_t controls the width of the wavepacket, and the complex-valued parameter γ_t determines the normalization and overall phase of the wavepacket.

In the Thawed Gaussian approximation, the potential function $V(x, t)$ is expanded in a quadratic Taylor series about the instantaneous center of the wavepacket:

$$V(x, t) \cong V_0 + V_1(x - x_t) + V_2(x - x_t)^2/2 \tag{7}$$

where $V_{0,1,2}$ are time-dependent coefficients given by $V_j = \partial^j V(x_t, t)/\partial x^j$ (i.e., the derivatives are evaluated at $x = x_t$). If $V(x, t)$ is at most a quadratic function of the coordinates, then the r.h.s. of Eq. (7) is simply an equivalent representation of $V(x, t)$. Otherwise, if the

potential is anharmonic, the r.h.s. is an approximation to $V(x,t)$ which is valid so long as the wavepacket is sufficiently narrow. An initially narrow wavepacket remains narrow for heavy mass particles or small $\hbar$, hence in the semiclassical limit GWD should become accurate for arbitrarily long times. Assuming this limit is achieved (or that the potential has no anharmonicities), we substitute Eqs. (6) and (7) into the time-dependent Schrödinger Equation (TDSE) and derive equations of motion for the parameters in the Gaussian, namely [1]:

$$\dot{x}_t(t) = p_t/m \tag{8}$$

$$\dot{p}_t(t) = -V_1 \tag{9}$$

$$\dot{\alpha}_t = -2\alpha_t^2/m - V_2/2 \tag{10}$$

$$\dot{\gamma}_t = i\hbar\alpha_t/m + p_t^2/2m - V_0 \tag{11}$$

The first two equations are just Hamilton's equations, i.e. in Thawed Gaussian Wavepacket Dynamics the position-space and momentum-space centers of the wavepacket evolve according to the laws of classical mechanics. The parameters α_t and γ_t also obey appropriate 1st order differential equations (which use x_t, p_t as input.) Numerical integration of the entire set of coupled 1st order differential equations is straightforward and fast. Extension to many cartesian degrees of freedom is straightforward.

3 Analysis of Driven Oscillator Problem

Using the GWD technique we can analyze the driven harmonic oscillator problem introduced in Section 1. The potential experienced by the oscillator is:

$$V(x,t) = \frac{1}{2}m\omega^2x^2 + f(t)x \tag{12}$$

where m is the oscillator mass (the reader should substitute $m \rightarrow m_x$ to connect to Fig. 1) and ω is its angular frequency (related to the spring force constant k by $\omega \equiv \sqrt{k/m}$). The relevant forcing function $f(t)$ for the collision-induced excitation problem of Section 1 is a pulse whose characteristics reflect the speed and mass of the projectile and the length scale of the interaction between the oscillator and the projectile atom.

We note further that a harmonic oscillator system in $v = 0$ is represented by a Gaussian wavepacket corresponding to $x_0 = 0$, $p_0 = 0$, $\alpha_0 = im\omega/2$ and $\gamma_0 = \frac{-i\hbar}{4}\ln(\frac{m\omega}{\pi\hbar})$. The evolution of the GWD parameters is as follows. First, $\alpha_t = \alpha_0$; in particular the wavepacket does not spread or contract with time (such a wavepacket is called a "coherent state"). Further, $\gamma_t = \gamma_0 + \omega t/2 + \int_0^t dt'[p_{t'}^2/2m - V_0(t')]$, i.e. the wavepacket develops a phase but the normalization is time-independent. Finally, x_t obeys Newton's equation for a driven harmonic oscillator (and of course $p_t = m\dot{x}_t$), namely:

$$\ddot{x}_t + \omega^2 x_t = f(t)/m \tag{13}$$

This differential equation can be explicitly integrated. If we are interested in asymptotic transition probabilities, it turns out that the central quantity we have to calculate is E_{cl}, the final energy of the oscillator after the collision is over. From the solution to Eq. (13), it follows directly that

$$E_{cl} = \frac{1}{2m}\left|\int_{-\infty}^{\infty} dt f(t) e^{i\omega t}\right|^2 \tag{14}$$

By plugging the explicit solutions for x_t, p_t, α_t and γ_t into the Gaussian wavepacket $\psi(x,t)$ and then performing the overlap integrals with the standard harmonic oscillator functions as indicated in Eq. (5), one finds a very simple expression for the probability that the collision induces a transition from the ground state $v = 0$ to final state v', namely:

$$P_{0\to v'} = e^{-\Gamma}\Gamma^{v'}/v'! \tag{15}$$

where Γ is the dimensionless ratio $\Gamma \equiv E_{cl}/\hbar\omega$. The transition probabilities indicated in Eq. (15) thus follow a Poisson distribution. Finally, we note that for the form of $f(t)$ adopted in Section 1 for the collinear atom-diatom collision, explicit evaluation of Γ yields:

$$\Gamma = \frac{\pi m_y v_0^2}{8\hbar\omega} e^{-\omega^2 L^2/2v_0^2} \tag{16}$$

4 Collisions with an Anharmonic Oscillator

Now let us make the seemingly innocent change that the oscillator is bound in a Morse potential,

$$V(x) = D(1 - e^{-ax})^2 \tag{17}$$

As is obvious from inspection, for small amplitude vibrations this potential behaves as a harmonic oscillator with effective force constant $k_{eff} = 2Da^2$. For larger amplitude motion, however, the particle senses *an*harmonic terms in the potential function. In classical mechanics, its trajectory is not longer sinusoidal. The quantum mechanical behavior of a wavepacket in a Morse potential can be rather exotic. In general, the shape does not remain Gaussian (except at short times). Both classical and quantal descriptions of the "kicked" Morse oscillator admit dissociation if enough energy is transferred to the oscillator coordinate.

As hinted in the above paragraph, the Gaussian Wavepacket Dynamics algorithm can fail badly for long-time motion in a Morse potential. For this reason we "bite the bullet" and utilize a numerical grid algorithm to integrate the time-dependent Schrödinger Equation in one spatial dimension. Details of the algorithm, which is a key tool in modern wavepacket methodology, are deferred until the next chapter. Here we study some results for the driven Morse oscillator. The large qualitative differences from the analogous harmonic oscillator problem that can arise under certain conditions motivate the careful study of grid methods below.

In Fig. 2 we show a wavepacket trajectory for $m_x = m_y = \hbar = 1$, $D = 12.5$, $a = 0.2$, $v_0 = 18$, and $L = 27$. The energy of excitation is high enough and the potential energy anharmonic enough that the wavepacket movie does not look anything like the dynamics of a coherent Gaussian wavepacket attained for the corresponding harmonic oscillator problem. The deviation from the harmonic oscillator model is even greater at very high collision energies - the oscillator system can dissociate.

To finish the analysis we show in Fig. 3 the analogous results for a harmonic oscillator well characterized by the effective frequency at the bottom of the Morse well studied in Fig. 2 above (namely, $\omega_{eff} = \sqrt{k_{eff}/m_x}$). Of course, the linearly driven harmonic oscillator remains in a Gaussian coherent state (does not spread). The particle is noticably more excited than the corresponding Morse oscillator for the same driving pulse.

References

[1] E.J. Heller, J. Chem. Phys. **62**, 1544 (1975); Accts. Chem. Res. **14**, 368 (1981).

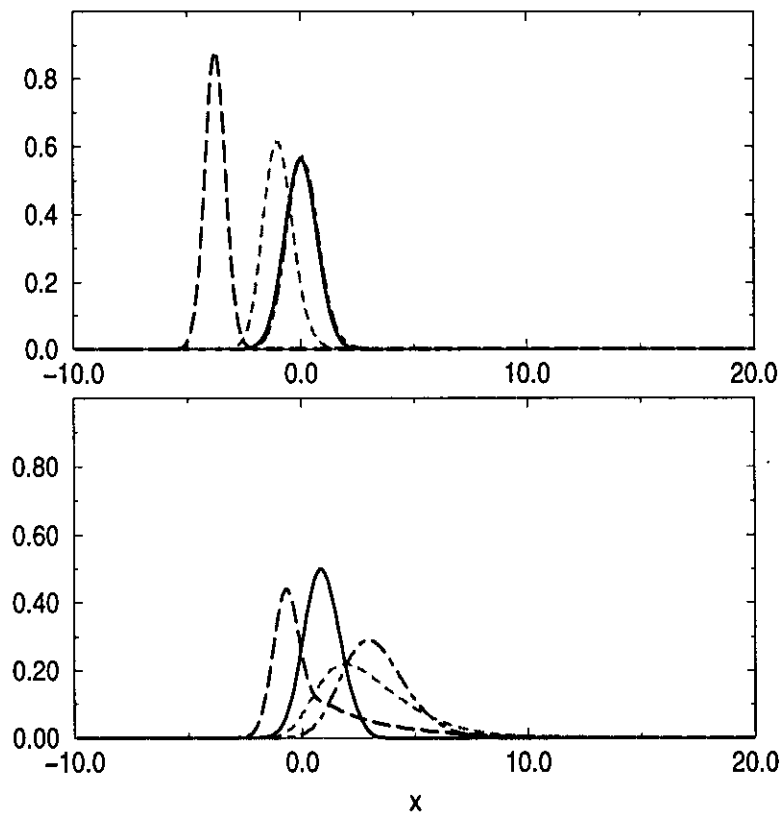

Figure 2: Probability density $|\psi(x,t)|^2$ vs x for driven Morse oscillator described in text. In top panel results are shown for times $t = 0, 1.5, 3.0, 4.5$ using solid, dot-dashed, dashed, and long dashed lines, respectively. In bottom panel results are shown for times $t = 6.0, 7.5, 9.0, 10.5$ using solid, dot-dashed, dashed, and long dashed lines, respectively.

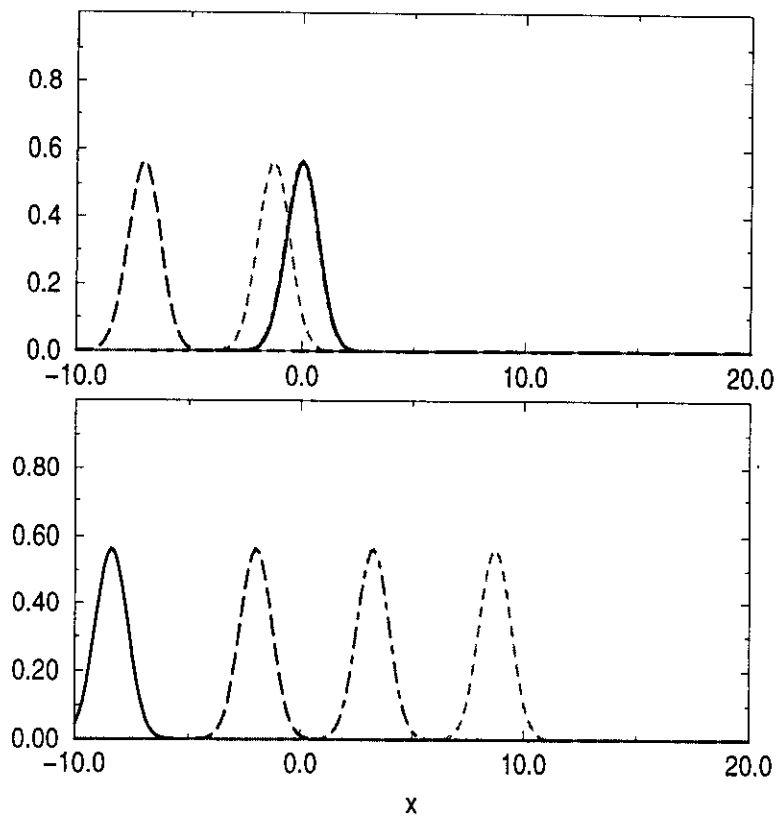

Figure 3: Probability density $|\psi(x,t)|^2$ vs x for driven harmonic oscillator described in text. In top panel results are shown for times $t = 0, 1.5, 3.0, 4.5$ using solid, dot-dashed, dashed, and long dashed lines, respectively. In bottom panel results are shown for times $t = 6.0, 7.5, 9.0, 10.5$ using solid, dot-dashed, dashed, and long dashed lines, respectively.

Chapt. 2: Numerical Grid Wavepacket Integrators

1 Grid Wavepacket Algorithms: SOD and Split Operator Methods

It is easy to convert the time-dependent Schrödinger Eq. (TDSE) into a finite difference equation which can be integrated on a computer [1]. If we discretize the wavepacket on a grid of evenly spaced position space points and use simple finite difference representations of the derivatives which appear in the TDSE, we arrive immediately at the update rule:

$$\frac{i\hbar}{\epsilon}\left[\psi_j(t+\epsilon)-\psi_j(t)\right]=\frac{-\hbar^2}{2m\delta^2}\left[\psi_{j+1}(t)-2\psi_j(t)+\psi_{j-1}(t)\right]+V_j(t)\psi_j(t) \tag{1}$$

Here $\psi(x_j,t)$ is denoted by $\psi_j(t)$, and analogously for $V(x_j,t)$; ϵ is the time step, and δ the spatial grid spacing. Now, given the packet at time t everywhere on the grid, the value of ψ at time $t+\epsilon$ can be computed.

In practice, wavepacket solutions of the TDSE oscillate rapidly in space and time, and the simple prescription just given is often unstable. To surmount these problems the following more sophisticated procedures are used.

First, all spatial derivatives are done by Fast Fourier Transform (FFT), rather than finite differencing. In particular, the current wavepacket ψ is fed into the FFT, which returns coefficients a_k in a Fourier series approximation to ψ:

$$\psi(x,t)=\sum_{k=-k_{max}}^{k_{max}} a_k e^{2\pi ikx/L} \tag{2}$$

This approximation to ψ can be differentiated analytically, e.g.

$$\frac{\partial^2\psi(x,t)}{\partial x^2}\cong\sum_{k=-k_{max}}^{k_{max}} -(2\pi k/L)^2 a_k e^{2\pi ikx/L} \tag{3}$$

To evaluate this approximation to $\partial^2\psi/\partial x^2$ at all grid points, just feed the new Fourier coefficients, $-(2\pi k/L)^2$, (backwards) through the FFT. A summary of the prescription for computing $\partial^n\psi/\partial x^n$ is thus:

(i) "FFT from real space to k space"

(ii) "multiply by $(ik)^n$ in k space"

(iii) "FFT back from k space to real space"

Now for the time derivative. Perhaps the simplest successful scheme is "Second Order Differencing" (SOD) [1]. To derive it, we note the formally exact solution $\psi(x, t+\epsilon) = \exp(-i\hat{H}\epsilon/\hbar)\psi(x,t)$, and consider evolution forwards and backwards by a small time ϵ:

$$\psi(x_j, t+\epsilon) = \psi(x_j,t) + (-i\epsilon/\hbar)\hat{H}\psi(x_j,t) + \frac{1}{2}(-i\epsilon/\hbar)^2\hat{H}^2\psi(x_j,t) \tag{4}$$

$$\psi(x_j, t-\epsilon) = \psi(x_j,t) + (i\epsilon/\hbar)\hat{H}\psi(x_j,t) + \frac{1}{2}(i\epsilon/\hbar)^2\hat{H}^2\psi(x_j,t) \tag{5}$$

Subtracting the second equation from the first, we obtain the SOD scheme:

$$\psi(x_j, t+\epsilon) - \psi(x_j, t-\epsilon) = (-2i\epsilon/\hbar)\hat{H}\psi(x_j,t) \tag{6}$$

Note that $\hat{H}\psi(x_j,t)$ can be accurately evaluated at all x_j by the methods discussed above. The advantage of the second order form Eq. (6) is that it is accurate through $O(\epsilon^2)$, while the first order form Eq. (1) is only accurate through order ϵ. SOD is a bit more involved since not only must the current wavepacket be stored but also the packet from the previous time step. (To start the algorithm, use the 1st order form for the first time step.)

Another elegant scheme is the "Split Operator Method" [2]. Denote the Hamiltonian as $\hat{H} = \hat{T} + \hat{V}$, with $\hat{T}$ the kinetic energy and $\hat{V}$ the potential (assumed to be a function of x and t). Although $\left[\hat{T}, \hat{V}\right] \neq 0$, for short times ϵ the "split operator" approximation:

$$\exp(-i\epsilon\hat{H}/\hbar) \cong \exp(-i\epsilon\hat{V}/2\hbar)\exp(-i\epsilon\hat{T}/\hbar)\exp(-i\epsilon\hat{V}/2\hbar) \tag{7}$$

is acceptable. In fact, it can be shown by direct expansion of the exponentials that the first error in the approximation is at $O(\epsilon^3)$. The Split Operator scheme takes full advantage of the FFT: First we operate on $\psi(x,t)$ with $\exp(-i\epsilon\hat{V}/2\hbar)$. This is multiplicative in real space, i.e. $\psi_j \rightarrow \exp(-i\epsilon V_j/2\hbar)\psi_j$. Now we operate on the new ψ with $\exp(-i\epsilon\hat{T}/\hbar)$. This operation is multiplicative in k space, so we use the FFT to transform to k space, multiply there, then FFT back to real space. Finally, we operate on the output of the Kinetic Energy propagation with $\exp(-i\epsilon\hat{V}/2\hbar)$ to obtain $\psi(x, t+\epsilon)$.

Basic properties of the exact solution include: If the Hamiltonian is Hermitian (the potential is real), norm is conserved. If the Hamiltonian is Hermitian and time-*in*dependent, then $< \psi(t)|\hat{H}^n|\psi(t) >$ is constant. In practice it is not hard to compute the first moment of $\hat{H}$ after each time step, hence norm and energy conservation can be monitored easily.

2 Examples of 1-d Grid Propagation

2.1 Tunneling through a Barrier

A good system for demonstrating the utility of numerical grid wavepacket propagation is tunneling through a barrier. In elementary textbooks this process is usually analyzed from a time-independent perspective. While such an analysis does indeed yield correct predictions for transmission and reflection probabilities, it cannot address the full range of issues associated with the dynamics of a wavepacket incident on a barrier. Time-dependent grid integrators provide considerable insight, as well as quantitative answers for measurable properties like scattering cross sections. [Fortunately, they are the *same* answers as obtained via time-independent analysis!]

First we have to define appropriate initial conditions for the wavefunction, and then solve the TDSE. We want to represent a free particle with prescribed initial momentum, incident (say, from the left) on a barrier. Intuitively, the nearest quantum analog to a classical particle is a localized wavepacket. Indeed, the notion of "scattering" implies that an event must take place: there must be a "before" state and an "after" state. To guarantee this we need to launch a localized wavepacket at the barrier at some time in the distant past.

Thus, consider an initial, normalized wavepacket of Gaussian form:

$$\psi(x,0) = [2\pi L_0^2]^{-1/4} \exp\left[-(x+x_0)^2/4L^2 + ip_0x/\hbar\right] .$$

This wavepacket is localized about $x = -x_0$ and has a width $\approx L$. An objection to identifying this state with an incident particle of momentum p_0 (or kinetic energy $E = p_0^2/2m$, m being the particle mass) is that it contains a distribution of momenta, or equivalently, it is not "monoenergetic". This objection can be met by increasing L until the momentum distribution becomes narrow. (It is easy to calculate that $< (p-p_0)^2 >= \hbar^2/L^2$.) By choosing x_0 sufficiently large (starting the particle far enough from the barrier), the necessary pre-collision localization can still be maintained.

Given the initial wavepacket just specified, the TDSE can be numerically integrated using the grid-methodology outlined in Sect. 1. Let us look at some movies of the scattering of a wavepacket from a square mound barrier, i.e., a potential which has the value V_0 in the region $-a/2 < x < a/2$ and is zero elsewhere.

For $m = \hbar = 1$ the trajectory of a wavepacket representing a particle with $E = 6$ and a square mound with $V_0 = 10$, $a = 0.6$ is shown in Fig. 1. The remarkable result is that although most of the wavepacket reflects (and, except for transient effects associated with the jarring

collision, retains its initially Gaussian shape), a part of the packet is transmitted through the barrier (again, recovering a Gaussian shape after it leaves the barrier region). For these particular collision conditions, 13% of the incident probability distribution permeates the barrier.

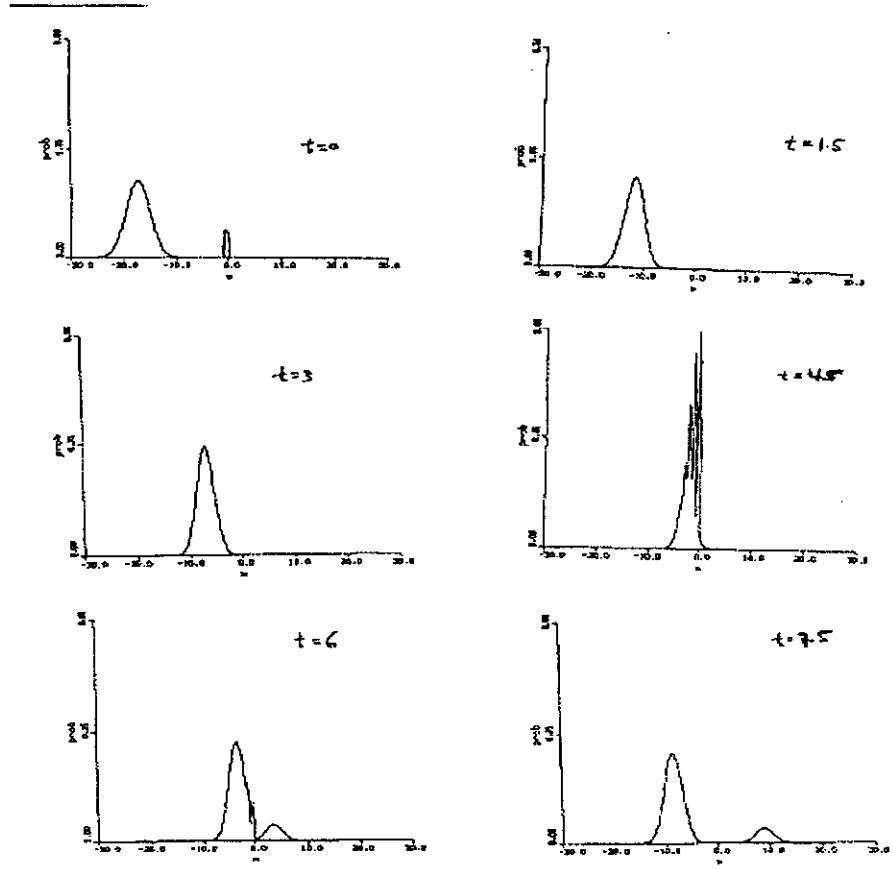

Figure 1: Wavepacket tunneling through a square mound barrier. Each panel shows probability density vs position at the indicated time. Position of barrier is shown in the first panel ($t = 0$). System parameters (see text) are $E/V_0 = 6/10$, $a = 0.6$, $\hbar = m = 1$.

To confirm the accuracy of these wavepacket results, it is instructive to compare to the formulae for transmission and reflection obtained by standard time-independent analysis. It turns out that for $E < V_0$ the transmission probability $|T|^2$ is given by the formula:

$$|T|^2 = \left[1 + \frac{\sinh^2(\kappa a)}{4(E/V_0)(1 - E/V_0)}\right]^{-1} \tag{8}$$

with $\kappa \equiv \sqrt{2m(V_0 - E)/\hbar}$. Thus, transmission increases monotonically with E for $E < V_0$. For $a = 0.6$, and $E/V_0 = 0.6$, Eq. 8 gives $|T|^2 = 0.12$, in reasonable agreement with the wavepacket movies shown above.

2.2 Absorbing Boundary Conditions for Grid Wavepacket Codes

A number of interesting quantum dynamics problems, such as the decay of a metastable state by tunneling through a confining barrier, have the feature that probability amplitude "dribbles" slowly out of the region of space where the system is (nearly) trapped. When the "dribble" hits the edge of the simulation box, it gets artificially reflected back into the box. This is undesirable. The simplest cure for this problem is to use a bigger box. However, there are always limits to computer storage, speed and user patience. Fortunately, the details of the dribble are usually not important. If we carefully "damp them out", this distortion of the actual quantum evolution of the system will have no effect on the behavior of the wavepacket in the important regions of space (for example, in the example of metastable decay, the region in and around the confining well). By applying "absorbing boundary conditions" we can eliminate the pieces of the wavepacket which have tunneled out of the well, are far away from it, and in the future will only go farther away still.

Here we discuss one simple strategy for "damping" outgoing wavepacket components which we do not need to follow explicitly, but wish to prevent from artificially reflecting back into the center of the grid after hitting the grid boundaries. In the one dimensional example of metastable decay with leakage through, say, the right-hand barrier, we choose a value of x, denoted x_d which is far to the right of the well region, but not all the way to the right-hand grid boundary. We then multiply the evolving wavepacket after each time step by the switching function

$$s(x) = \left[1 + e^{a(x-x_d)}\right]^{-1} \tag{9}$$

This function switches smoothly from the value $s = 1$ to $s = 0$ as x increases through x_d. The width of the switching region is roughly a^{-1}. For sufficiently small a the switching will take place gradually enough that no artificial reflection of outgoing pieces of the wavepacket back into the center of the grid will occur. It should be checked that important quantities associated with the wavepacket dynamics in the center of the grid do not change as the box size and x_d are increased, and the value of a is reduced.

3 Grid Wavepacket Dynamics in Several Cartesian Dimensions

Extension of the 1-d grid algorithms considered above to propagate wavepackets in two or more cartesian dimensions is quite straightforward in principle. The major problem is that the computational effort required scales roughly *geometrically* with spatial dimensionality of the system, so we simply run out of storage space and cpu time after 3-4 spatial dimensions. Nevertheless, exact grid integrators in 2-4 spatial coordinates are extremely useful. Even in 2-d, one can begin to study effects of *coupling* between dynamical degrees of freedom, at a level of detail, reliability and flexibility which did not exist before grid methods came of age in the 1980's.

An important point to note is that for a multidimensional system, if the potential is separable and the initial wavepacket factors into a product (one factor for each degree of freedom), then the problem of propagating the wavepacket separates into a collection of uncoupled 1-d problems. To be more specific, consider a system with two dynamical degrees of freedom x and y. Further, let us assume that the kinetic energy has the usual form for cartesian coordinates, $\hat{T} = \hat{T}_x + \hat{T}_y$, with $\hat{T}_x = \frac{-\hbar^2}{2m}\frac{\partial^2}{\partial x^2}$, and analogously for $\hat{T}_y$.

Then, if $V(x,y) = V_x(x) + V_y(y)$, *and* if $\psi(x,y,t=0) = \psi_x(x)\psi_y(y)$, it follows that $\psi(x,y,t) = \psi_x(x,t)\psi_y(y,t)$, where $\psi_x(x,t)$ satisfies the 1-d TDSE

$$i\hbar\partial\psi_x(x,t)/\partial t = \left[\hat{T}_x + V_x(x)\right]\psi_x(x,t) \tag{10}$$

subject to the initial condition $\psi_x(x,0) = \psi_x(x)$.

In general, $V(x,y)$ is not separable, and the solution of a coupled 2-d TDSE must be computed. This can be done on a two dimensional spatial grid.

All of the basic strategies, e.g. SOD and Split Operator methods, discussed in the 1-d case work for the multidimensional as well. Operators involving the position of the degrees of freedom [like $V(x,y)$] act on the wavefunction via local multiplication, as in 1-d. The most difficult part is again the operation of momentum operators (e.g., the kinetic energy operator) on the wavefunction. Fortunately, these operators are still "local in k space". That is, if we approximate $\psi(x,y,t)$ as a Fourier series (with periodicity reflecting the box length $L_{x,y}$ in each direction):

$$\psi(x,y,t) = \sum_{k_x=-k_{max}}^{k_{max}} \sum_{k_y=-k_{max}}^{k_{max}} a_{k_x,k_y} \exp(2\pi i k_x x/L_x) \exp(2\pi i k_y x/L_y) \ , \tag{11}$$

derivative operations on this form are easy, e.g.:

$$\frac{\partial^{m_x+m_y}\psi(x,y,t)}{\partial x^{m_x}\partial y^{m_y}} = \sum_{k_x=-k_{max}}^{k_{max}} \sum_{k_y=-k_{max}}^{k_{max}} \bar{a}_{k_x,k_y} \exp(2\pi i k_x x/L_x) \exp(2\pi i k_y x/L_y) \qquad (12)$$

with

$$\bar{a}_{k_x,k_y} \equiv (2\pi i k_x/L_x)^{m_x} (2\pi i k_y/L_y)^{m_y} a_{k_x,k_y} \qquad (13)$$

The evaluation of derivatives by this strategy is greatly aided by the existence of two (and higher!) dimensional FFT routines. The procedure is the same as in 1-d, namely for a 2-d problem, (i) feed the coordinate space grid to the 2-d FFT routine, (ii) modify the output Fourier coeffs. as indicated in Eq. (13) (for the operator $\partial^{m_x+m_y}/\partial^{m_x}\partial^{m_y}$), (iii) FFT back to coordinate space.

Grid-integration routines are the "bread and butter" of quantum dynamicists studying small systems. Unfortunately, the systems have to be *very* small. Computational effort (both cpu and storage) grows *geometrically* with dimension. If it takes 100 grid points to span the relevant region of a 1-d configuration space, then it will take 100^2 to span a 2-d configuration space, 100^3 for 3-d, etc. Depending on the computer resources and perserverance of the researcher, 3-4 spatial degrees of freedom is the upper limit for exact wavepacket calculations using general purpose grid-integrators.

Hence, approximate methods are still widely utilized. One of these, the multidimensional generalization of Gaussian Wavepacket Dynamics, is discussed next.

References

[1] R. Kosloff, J. Phys. Chem. **92**, 2087 (1988).

[2] M.D. Feit, J.A. Fleck and A. Steiger, J. Comput. Phys. **47** 412, (1982).